

# An Effective Semi-blind Receiver in Cooperative MIMO Relay Systems



Hong-Yan Sun<sup>1\*</sup>, Meng Han<sup>2</sup>, Si-Yu Ye<sup>2</sup>

<sup>1</sup> School of Physics and Electronic Engineering, Heze University, Heze, Shandong 274015, China  
shy02@163.com

<sup>2</sup> School of Information and Communication Engineering, Communication University of China,  
Beijing, Beijing 100024, China  
{hanmengcuc, yesiyucuc}@sina.com

Received 28 July 2019; Revised 13 December 2019; Accepted 20 January 2020

**Abstract.** In this paper, a tensor-based semi-blind receiver model is considered for cooperative multiple input multiple output (MIMO) relay systems. The proposed receiver allows a joint symbol and channel estimation without requiring pilot sequences for channel state information (CSI) acquisition. A Tucker-2 tensor model with special structure is constructed. Then we utilize the decomposition uniqueness of the tensor model and design an efficient tensor fitting algorithm. By making full use of the gain of cooperative diversity, the proposed receiver can effectively estimate the information symbols transmitted by the source node and channel matrices even when the number of antennas of the relay and destination nodes is very small. Besides, compared with the existing ALS receiver, the proposed receiver has better signal and channel estimation performance. Simulation results verify the effectiveness of the proposed semi-blind receiver.

**Keywords:** joint estimation, MIMO relay, semi-blind receiver, Tucker-2 model

## 1 Introduction

Multiple-input multiple-output (MIMO) technology [1] uses multiple antennas to transmit and receive signals independently at transmitter and receiver end. MIMO technology achieves the huge growth of spectral efficiency without increasing the occupancy of spectral resources and transmission power. Cooperative relay technology [2] improves capacity and throughput of wireless systems. Their combination can make full use of spatial diversity and further improve the performance of the system. At present, MIMO relay system has attracted wide attention from academia and industry [3-6].

A lot of studies on MIMO relay assume that the system has known channel matrices or accurate channel state information (CSI). However, in practical communication systems, they are unknown. The channel estimation and CSI acquisition of MIMO relays are fairly important.

In many fields, such as radar, mobile communications, sonar and seismology, their information symbols have multidimensional structures that can be processed by applying the tensor-based approach [7]. According to the knowledge of matrix theory, the matrix decomposition is not unique when the rank of the matrix is greater than one without any additional constraints. While the tensor decomposition is essentially unique, which makes it more valuable in applications. It is a commonly used technique for channel estimation in MIMO relay systems.

For MIMO relay systems, a two-stage channel estimation method is proposed in [8]. This method achieves better channel matrix estimation by optimizing pilot design. In [9], a channel estimation method based on parallel factor (PARAFAC) [10] is proposed. This method can jointly estimate the two-hop channel matrix. A low complexity alternating least squares (ALS) fitting algorithm [11] is also proposed

---

\* Corresponding Author

in [9]. However, works [9] and [10] need to know the first row or column of one factor matrix to remove scaling ambiguity. In [12], the PARATUCK2 model [13] is introduced to the two-hop cooperative MIMO relay system. By building the PARATUCK2 model, which is constructed by the relaying auxiliary link signals received by the sink, we can realize the joint estimation of transmitted symbols and the channels from source to relay station and relay to sink. In [14], for multi-user MIMO relay systems, the fast convergence of Levenberg-Marquardt (LM) fitting algorithm is used to improve the efficiency of channel estimation. The work [15] utilizes tensor space-time (TST) coding scheme to encode transmit signals. Therefore, the received signals can be modeled as the Tucker-2 model. And then, joint channel and symbol estimation are achieved by using optimized LM algorithm. Recently, a closed-form tensor-based estimation algorithm is proposed in [16] without resorting to pilots by using double Khatri–Rao space-time (KRST) coding structure. The computational complexity of this algorithm is greatly reduced. In [17], a simplified KRST coding scheme is used for a one-way multi-hop MIMO relay system with  $K$  relays. The received signals are decomposed as  $K + 1$  PARAFAC models. And then, a sequential closed-form semi-blind receiver is proposed. In [18], the TST coding scheme is utilized and two closed-form semi-blind receivers are proposed for the two-way relay system. The received signals are modeled as a block Tucker-2 model at the relay and a Tucker-2 model at the sources. It is important to note that one of the proposed receivers can be applied to channels without channel reciprocity.

The method in [8] takes up spectral resources due to the use of pilots. The ALS algorithm used in [9] and [12] is a classical algorithm for fitting multidimensional matrix models. It can guarantee monotonic convergence and is easy to carry out. However, the ALS algorithm exhibits convergence problem if ill-conditioned factor matrices exist. Though LM fitting algorithm in [14] and [15] can overcome convergence problem existing in ALS algorithm, it has high complexity in each iteration. Closed-form algorithms in [16-17], and [18] have low complexity. However, since these closed-form algorithms can not utilize cooperative diversity, they have low estimation performance.

In this paper, we propose an effective semi-blind receiver for cooperative MIMO relay systems. Firstly, the proposed receiver encodes the transmitted information symbols in three-dimensional space-time codes at the source node. The source transmits information signals to the relay and also to the destination. Secondly, the relay amplifies the received signals and forwards them to the destination. Thirdly, all the information of the relay link and the direct link is collated and the Tucker-2 tensor model is constructed at the destination node. Finally, an efficient tensor fitting algorithm is proposed to fit the constructed Tucker-2 model for jointly estimating information symbols and the channel matrices of the two links. The contributions of this paper are as follows. (1) Compared with the commonly used PARAFAC model, the Tucker-2 model constructed in this paper needs less prior information to eliminate scale ambiguity. (2) Compared with the existing ALS receivers, the proposed algorithm does not need to calculate the pseudo-inverse of matrix at each iteration. Therefore, it has low complexity. (3) Because the receiver can make full use of the cooperative diversity gains, it has high estimation performance, and the proposed receiver still has good estimation performance even in the strong correlation scenario.

The rest of this paper is organized as follows. Section 2 gives a brief introduction to the Tucker model used in this paper. The proposed two-hop MIMO relay system model is presented in Section 3. In Section 4, the Tucker-2 tensor model is constructed. Section 5 develops the proposed channel estimation algorithm. Numerical results are illustrated in Section 6. Conclusions are drawn in Section 7.

#### Notations:

Lower-case  $(a, b, \dots)$ , boldface lower-case  $(\mathbf{a}, \mathbf{b}, \dots)$ , boldface capital  $(\mathbf{A}, \mathbf{B}, \dots)$ , and calligraphic letters  $(\mathcal{A}, \mathcal{B}, \dots)$  denote scalars, column vectors, matrices, and tensors, respectively.  $\mathbf{A}^T$ ,  $\mathbf{A}^H$ ,  $\mathbf{A}^\dagger$ ,  $\mathbf{A}_{i\cdot}$ , and  $\mathbf{A}_{\cdot m}$  are the transpose, the Hermitian transpose, the Moore-Penrose pseudo-inverse, the  $i$ th row, and the  $m$ th column of  $\mathbf{A} \in \mathbb{C}^{L \times M}$ , respectively. Frobenius norm is denoted by  $\|\cdot\|_F$ . The identity matrix of dimensions  $N \times N$  is represented by  $\mathbf{I}_N$ .  $\mathbf{e}_n^{(N)}$  denotes the  $n$ -th canonical vector of the Euclidean space  $\mathbb{R}^N$ . The Kronecker product, Khatri-Rao product, and outer product are denoted by  $\otimes$ ,  $\circ$ , and  $\odot$ , respectively.  $\mathbf{A}_{i..} \in \mathbb{C}^{J \times K}$ ,  $\mathbf{A}_{\cdot j} \in \mathbb{C}^{J \times K}$ , and  $\mathbf{A}_{\cdot\cdot k} \in \mathbb{C}^{I \times J}$  denote the horizontal, lateral, and frontal slices of third-order tensor  $\mathcal{A} \in \mathbb{C}^{I \times J \times K}$  with entry  $a_{i,j,k}$ , respectively.

## 2 Tucker Model

The Tucker model has been widely used in channel estimation and data analysis fields [19] and attracted great attention. We give a brief introduction to the Tucker model used in this paper. For the Tucker model of an  $N$ -th order tensor  $\mathcal{Z} \in \mathbb{C}^{I_1 \times \dots \times I_N}$ , its mode- $n$  product form is defined as [20]:

$$\begin{aligned} \mathcal{Z} &= \mathcal{F} \times_1 \mathbf{A}^{(1)} \times_2 \mathbf{A}^{(2)} \times_3 \dots \times_N \mathbf{A}^{(N)} \\ &= \mathcal{F} \times_{n=1}^N \mathbf{A}^{(n)}, \end{aligned} \quad (1)$$

where  $\mathbf{A}^{(n)} \in \mathbb{C}^{I_n \times R_n}$  and  $\mathcal{F} \in \mathbb{C}^{R_1 \times \dots \times R_N}$  are matrix factor and core tensor of the Tucker model for  $n=1, \dots, N$ , respectively.  $\mathcal{F} \times_n \mathbf{A}^{(n)}$ , standing for the mode- $n$  product of  $\mathcal{F}$  and  $\mathbf{A}^{(n)}$ , gives a tensor  $\mathcal{Y} \in \mathbb{C}^{R_1 \times \dots \times R_{n-1} \times I_n \times R_{n+1} \times \dots \times R_N}$  such that [21]

$$y_{i_1, \dots, i_{n-1}, i_n, i_{n+1}, \dots, i_N} = \sum_{r_n=1}^{R_n} a_{i_n, r_n}^{(n)} g_{i_1, \dots, i_{n-1}, r_n, i_{n+1}, \dots, i_N}, \quad (2)$$

where  $y_{i_1, \dots, i_{n-1}, i_n, i_{n+1}, \dots, i_N}$ ,  $a_{i_n, r_n}^{(n)}$ , and  $g_{i_1, \dots, i_{n-1}, r_n, i_{n+1}, \dots, i_N}$  are typical elements of  $\mathcal{Y}$ ,  $\mathbf{A}^{(n)}$ , and  $\mathcal{F}$  for  $i_n=1, \dots, I_n$ , respectively. The mode- $n$  matrix unfolding expression can be represented by

$$\mathbf{Y}_n = \mathbf{A}^{(n)} \mathbf{G}_n, \quad (3)$$

where  $\mathbf{G}_n$  and  $\mathbf{Y}_n$  are mode- $n$  matrices corresponding to  $\mathcal{F}$  and  $\mathcal{Y}$ .

The definition (1) can also be expressed as the form of the outer products as follows:

$$\mathcal{Z} = \sum_{r_1=1}^{R_1} \dots \sum_{r_N=1}^{R_N} g_{r_1, \dots, r_N} \bigcirc_{n=1}^N \mathbf{A}_{\cdot r_n}^{(n)}, \quad (4)$$

in which  $\mathbf{A}_{\cdot r_n}^{(n)} = \sum_{i_n=1}^{I_n} a_{i_n, r_n}^{(n)} \mathbf{e}_{i_n}^{(I_n)}$ . Using the scalar representation, this model can be written as follows:

$$\begin{aligned} x_{i_1, \dots, i_N} &= \sum_{r_1=1}^{R_1} \dots \sum_{r_N=1}^{R_N} g_{r_1, \dots, r_N} \left( a_{i_1, r_1}^{(1)} \times \dots \times a_{i_N, r_N}^{(N)} \right) \\ &= \sum_{r_1=1}^{R_1} \dots \sum_{r_N=1}^{R_N} g_{r_1, \dots, r_N} \prod_{n=1}^N a_{i_n, r_n}^{(n)}, \end{aligned} \quad (5)$$

where  $x_{i_1, \dots, i_N}$  is a typical element of  $\mathcal{Z}$ .

As is known to all, different models can be deduced from the Tucker model. For example, the Tucker- $(N - N_1)$  or named Tucker- $(N_1, N)$  models [13], which correspond to the situation that  $N - N_1$  loading matrices are identity matrices. For the Tucker-2 model,  $N=3$ ,  $N_1=2$ ,  $\mathbf{A}^{(3)} = \mathbf{I}_{I_3}$  and  $R_3 = I_3$ . Then formulas (1) and (5) become

$$\begin{aligned} \mathcal{Z} &= \mathcal{F} \times_1 \mathbf{A}^{(1)} \times_2 \mathbf{A}^{(2)} \times_3 \mathbf{I}_{I_3} \\ &= \mathcal{F} \times_{n=1}^2 \mathbf{A}^{(n)}, \end{aligned} \quad (6)$$

$$\begin{aligned}
 x_{i_1, i_2, i_3} &= \sum_{r_1=1}^{R_1} \sum_{r_2=1}^{R_2} \sum_{r_3=1}^{R_3} g_{r_1, r_2, r_3} \prod_{n=1}^3 a_{i_n, r_n}^{(n)} \\
 &= \sum_{r_1=1}^{R_1} \sum_{r_2=1}^{R_2} g_{r_1, r_2, r_3} a_{i_1, r_1}^{(1)} a_{i_2, r_2}^{(2)}.
 \end{aligned} \tag{7}$$

### 3 System Model

We consider a two-hop cooperative relay system with a source node, a destination node, and a relay as shown in Fig. 1. The source and destination nodes are equipped with  $N_S$  and  $N_D$  antennas, respectively. While the relay is equipped with  $N_{R_1}$  receive antennas and  $N_{R_2}$  transmit antennas.  $\mathbf{H}^{(SR)} \in \mathbb{C}^{N_{R_1} \times N_S}$ ,  $\mathbf{H}^{(RD)} \in \mathbb{C}^{N_D \times N_{R_2}}$  and  $\mathbf{H}^{(SD)} \in \mathbb{C}^{N_D \times N_S}$  are the channel matrices with entries  $h_{n_{R_1}, n_S}^{(SR)}$ ,  $h_{n_D, n_{R_2}}^{(RD)}$ , and  $h_{n_D, n_S}^{(SD)}$  from the source to the relay, the relay to the destination, and the source to the destination, respectively. In addition,  $n_s = 1, \dots, N_S$ ,  $n_D = 1, \dots, N_D$ ,  $n_{R_1} = 1, \dots, N_{R_1}$ , and  $n_{R_2} = 1, \dots, N_{R_2}$ . Assuming that the relay works in half-duplex mode, the total transmission time is divided into two phases. In the first phase, information signals are transmitted from the source to the destination and also to the relay. In the second phase, relay forwards the amplified signals to the destination while the source is silent.

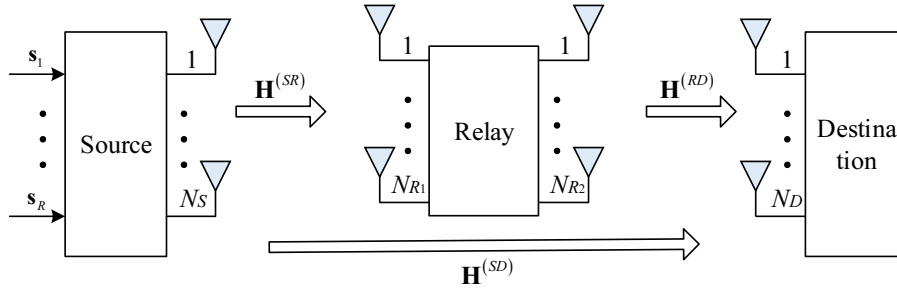


**Fig. 1.** The proposed two-hop MIMO relay system model

Each information symbol  $s_{r,m}$  is coded by a three-dimensional extended code  $w_{n_s, r, k}$  at the source end, where  $r = 1, \dots, R$ ,  $m = 1, \dots, M$ ,  $k = 1, \dots, K$ , and  $R, M, K$  denote the number of data streams, time-blocks, and slices, respectively.

Considering the  $m$ -th time-block, the transmitted signal on  $n_s$ -th antenna in the  $k$ -th slice is given by

$$b_{n_s, m, k} = \sum_{r=1}^R w_{n_s, r, k} s_{r, m}, \tag{8}$$

where  $s_{r,m}$  is the  $(r, m)$ -th entry of signal  $\mathbf{S} \in \mathbb{C}^{R \times M}$ ,  $w_{n_s, r, k}$  and  $b_{n_s, m, k}$  are typical elements of three-dimensional extended code tensor  $\mathscr{W} \in \mathbb{C}^{N_S \times R \times K}$ , and the transmitted signal tensor  $\mathscr{B} \in \mathbb{C}^{N_S \times M \times K}$ , respectively.

In the first phase, the received signals of the  $n_{R_1}$ -th relay antenna and the  $n_D$ -th destination antenna can be written as

$$x_{n_{R_1}, m, k}^{(SR)} = \sum_{n_s=1}^{N_S} \sum_{r=1}^R h_{n_{R_1}, n_s}^{(SR)} w_{n_s, r, k} s_{r, m} + v_{n_{R_1}, m, k}^{(SR)}, \tag{9}$$

$$x_{n_D, m, k}^{(SD)} = \sum_{n_s=1}^{N_S} \sum_{r=1}^R h_{n_D, n_s}^{(SD)} w_{n_s, r, k} s_{r, m} + v_{n_D, m, k}^{(SD)}, \tag{10}$$

where  $x_{n_{R_1},m,k}^{(SR)}$  and  $x_{n_D,m,k}^{(SD)}$  are typical elements of the received signal tensors  $\mathcal{X}^{(SR)} \in \mathbb{C}^{N_{R_1} \times M \times K}$  and  $\mathcal{X}^{(SD)} \in \mathbb{C}^{N_D \times M \times K}$  at the relay and destination nodes in the first phase, respectively,  $v_{n_{R_1},m,k}^{(SR)}$  and  $v_{n_D,m,k}^{(SD)}$  are corresponding typical elements of noise tensors  $\mathcal{V}^{(SR)} \in \mathbb{C}^{N_{R_1} \times M \times K}$  and  $\mathcal{V}^{(SD)} \in \mathbb{C}^{N_D \times M \times K}$ .

In the second phase, the received signals of the  $n_D$ -th destination antenna can be written as

$$\begin{aligned} x_{n_D,m,k}^{(SRD)} &= \sum_{n_{R_2}=1}^{N_{R_2}} \sum_{n_{R_1}=1}^{N_{R_1}} h_{n_D,n_{R_2}}^{(RD)} f_{n_{R_2},n_{R_1}} x_{n_{R_1},m,k}^{(SR)} + v_{n_D,m,k}^{(RD)} \\ &= \sum_{n_{R_2}=1}^{N_{R_2}} \sum_{n_{R_1}=1}^{N_{R_1}} \sum_{n_S=1}^{N_S} \sum_{r=1}^R h_{n_D,n_{R_2}}^{(RD)} f_{n_{R_2},n_{R_1}} h_{n_{R_1},n_S}^{(SR)} w_{n_S,r,k} s_{r,m} \\ &\quad + \sum_{n_{R_2}=1}^{N_{R_2}} \sum_{n_{R_1}=1}^{N_{R_1}} h_{n_D,n_{R_2}}^{(RD)} f_{n_{R_2},n_{R_1}} v_{n_{R_1},m,k}^{(SR)} + v_{n_D,m,k}^{(RD)}, \end{aligned} \quad (11)$$

where  $f_{n_{R_2},n_{R_1}}$  is the  $(n_{R_2}, n_{R_1})$ -th entry of the amplification coefficient matrix  $\mathbf{F} \in \mathbb{C}^{N_{R_2} \times N_{R_1}}$  at the relay node,  $x_{n_D,m,k}^{(SRD)}$  and  $v_{n_D,m,k}^{(RD)}$  are typical elements corresponding to the received signal tensor  $\mathcal{X}^{(SRD)} \in \mathbb{C}^{N_D \times M \times K}$  at the destination node in the second phase and the noise tensor  $\mathcal{V}^{(RD)} \in \mathbb{C}^{N_D \times M \times K}$ , respectively.

The matrix expression of (10) and (11) are

$$\mathbf{X}_{\cdot,k}^{(SD)} = \mathbf{H}^{(SD)} \mathbf{W}_{\cdot,k} \mathbf{S} + \mathbf{V}_{\cdot,k}^{(SD)}, \quad (12)$$

$$\mathbf{X}_{\cdot,k}^{(SRD)} = \mathbf{H}^{(RD)} \mathbf{F} \mathbf{H}^{(SR)} \mathbf{W}_{\cdot,k} \mathbf{S} + \mathbf{H}^{(RD)} \mathbf{F} \mathbf{V}_{\cdot,k}^{(SR)} + \mathbf{V}_{\cdot,k}^{(RD)}, \quad (13)$$

where  $\mathbf{X}_{\cdot,k}^{(SD)} \in \mathbb{C}^{N_D \times M}$ ,  $\mathbf{X}_{\cdot,k}^{(SRD)} \in \mathbb{C}^{N_D \times M}$ ,  $\mathbf{W}_{\cdot,k} \in \mathbb{C}^{N_S \times R}$ ,  $\mathbf{V}_{\cdot,k}^{(SD)} \in \mathbb{C}^{N_D \times M}$ ,  $\mathbf{V}_{\cdot,k}^{(SR)} \in \mathbb{C}^{N_{R_1} \times M}$ , and  $\mathbf{V}_{\cdot,k}^{(RD)} \in \mathbb{C}^{N_D \times M}$  are  $k$ -th frontal slices of  $\mathcal{X}^{(SD)}$ ,  $\mathcal{X}^{(SRD)}$ ,  $\mathcal{W}$ ,  $\mathcal{V}^{(SD)}$ ,  $\mathcal{V}^{(SR)}$ , and  $\mathcal{V}^{(RD)}$ , respectively.

#### 4 Construction of Tensor Model

(12) and (13) are stacked and processed, then we get

$$\mathbf{X}_{\cdot,k}^{(CP)} = \mathbf{H}^{(CP)} \mathbf{W}_{\cdot,k} \mathbf{S} + \mathbf{V}_{\cdot,k}^{(CP)}, \quad (14)$$

where

$$\mathbf{H}^{(CP)} = \begin{bmatrix} \mathbf{H}^{(SRD)} \\ \mathbf{H}^{(SD)} \end{bmatrix} \in \mathbb{C}^{2N_D \times N_S}, \quad (15)$$

$$\mathbf{H}^{(SRD)} = \mathbf{H}^{(RD)} \mathbf{F} \mathbf{H}^{(SR)} \in \mathbb{C}^{N_D \times N_S}, \quad (16)$$

$$\mathbf{X}_{\cdot,k}^{(CP)} = \begin{bmatrix} \mathbf{X}_{\cdot,k}^{(SRD)} \\ \mathbf{X}_{\cdot,k}^{(SD)} \end{bmatrix} \in \mathbb{C}^{2N_D \times M}, \quad (17)$$

and

$$\mathbf{V}_{\cdot,k}^{(CP)} = \begin{bmatrix} \mathbf{H}^{(RD)} \mathbf{F} \mathbf{V}_{\cdot,k}^{(SR)} + \mathbf{V}_{\cdot,k}^{(RD)} \\ \mathbf{V}_{\cdot,k}^{(SD)} \end{bmatrix} \in \mathbb{C}^{2N_D \times M}. \quad (18)$$

$\mathbf{X}_{\cdot,k}^{(CP)}$  and  $\mathbf{V}_{\cdot,k}^{(CP)}$  are  $k$ -th frontal slices of  $\mathcal{X}^{(CP)} \in \mathbb{C}^{2N_D \times M \times K}$  and  $\mathcal{V}^{(CP)} \in \mathbb{C}^{2N_D \times M \times K}$ , respectively.

Formula (14) can be written in the following scalar form

$$x_{n_D, m, k}^{(CP)} = \sum_{n_s=1}^{N_s} \sum_{r=1}^R h_{n_D, n_s}^{(CP)} w_{n_s, r, k} s_{r, m} + v_{n_D, m, k}^{(CP)}, \quad (19)$$

where  $h_{n_D, n_s}^{(CP)}$  is  $(n_{R_2}, n_{R_1})$ -th entry of  $\mathbf{H}^{(CP)}$ ,  $x_{n_D, m, k}^{(CP)}$  and  $v_{n_D, m, k}^{(CP)}$  are typical elements of  $\mathcal{X}^{(CP)}$  and  $\mathcal{Y}^{(CP)}$ .

It can be seen that formula (19) is a Tucker-2 model with noise. According to the decomposition feature of Tucker-2 model, we can get

$$\mathbf{X}_1^{(CP)} = (\mathbf{S}^T \otimes \mathbf{H}^{(CP)}) \mathbf{G}_1 + \mathbf{V}_1^{(CP)}, \quad (20)$$

$$\mathbf{X}_2^{(CP)} = (\mathbf{H}^{(CP)} \otimes \mathbf{S}^T) \mathbf{G}_2 + \mathbf{V}_2^{(CP)}, \quad (21)$$

where

$$\mathbf{G}_1 = [\text{vec}(\mathbf{W}_{\cdot 1}), \dots, \text{vec}(\mathbf{W}_{\cdot K})] \in \mathbb{C}^{N_s R \times K}, \quad (22)$$

$$\mathbf{V}_1^{(CP)} = [\text{vec}(\mathbf{V}_{\cdot 1}), \dots, \text{vec}(\mathbf{V}_{\cdot K})] \in \mathbb{C}^{N_D M \times K}, \quad (23)$$

$$\mathbf{G}_2 = [\text{vec}(\mathbf{W}_{\cdot 1}^T), \dots, \text{vec}(\mathbf{W}_{\cdot K}^T)] \in \mathbb{C}^{N_s R \times K}, \quad (24)$$

$$\mathbf{V}_2^{(CP)} = [(\text{vec}(\mathbf{V}_{\cdot 1}^T))^T, \dots, (\text{vec}(\mathbf{V}_{\cdot K}^T))^T] \in \mathbb{C}^{N_D M \times K}. \quad (25)$$

## 5 The Proposed Fitting Algorithm

According to (20) and (21), if matrix  $\mathbf{G}_1$  and  $\mathbf{G}_2$  have full row ranks, then we have

$$\begin{aligned} \mathbf{Y}_1 &= \mathbf{X}_1^{(CP)} \mathbf{G}_1^\dagger = (\hat{\mathbf{S}}^T \otimes \hat{\mathbf{H}}^{(CP)}) \\ &= \begin{bmatrix} \mathbf{Y}_1^{(1,1)} & \dots & \mathbf{Y}_1^{(1,R)} \\ \vdots & \ddots & \vdots \\ \mathbf{Y}_1^{(N_D,1)} & \dots & \mathbf{Y}_1^{(N_D,R)} \end{bmatrix} \in \mathbb{C}^{MN_D \times RN_s}, \end{aligned} \quad (26)$$

$$\begin{aligned} \mathbf{Y}_2 &= \mathbf{X}_2^{(CP)} \mathbf{G}_2^\dagger = (\hat{\mathbf{H}}^{(CP)} \otimes \hat{\mathbf{S}}^T) \\ &= \begin{bmatrix} \mathbf{Y}_2^{(1,1)} & \dots & \mathbf{Y}_2^{(1,N_s)} \\ \vdots & \ddots & \vdots \\ \mathbf{Y}_2^{(N_D,1)} & \dots & \mathbf{Y}_2^{(N_D,N_s)} \end{bmatrix} \in \mathbb{C}^{N_D M \times N_s R}, \end{aligned} \quad (27)$$

where  $\mathbf{Y}_1^{(n,r)} \triangleq (\hat{\mathbf{S}}^T \otimes \hat{\mathbf{H}}^{(CP)})^{(n,r)} = \hat{s}_{r,n} \hat{\mathbf{H}}^{(CP)}$  and  $\mathbf{Y}_2^{(n_D, n_s)} \triangleq (\hat{\mathbf{H}}^{(CP)} \otimes \hat{\mathbf{S}}^T)^{(n_D, n_s)} = h_{n_D, n_s}^{(CP)} \hat{\mathbf{S}}^T$ .  $\mathbf{G}_1$  and  $\mathbf{G}_2$  have full row ranks, i.e.  $K \geq RN_s$ . Comparing (20), (21) with (26), (27), it can be seen that the dimension of  $\mathbf{Y}_1$  is less than or equal to that of  $\mathbf{X}_1^{(CP)}$ , and the dimension of  $\mathbf{Y}_2$  is less than or equal to that of  $\mathbf{X}_2^{(CP)}$ . In order to reduce the computational complexity, according to the special structure of Kronecker product,  $\hat{\mathbf{S}}$  and  $\hat{\mathbf{H}}$  can be estimated jointly from (26) and (27) by alternating iteration method. An advantage of this method is that it does not need iterative pseudo-inverse calculation. Thus there will be no ill-conditioned

conditions resulting in slow convergence in the fitting process. The procedures of the proposed algorithm are as following:

**Step 1:** Formulas (20) and (21) are right multiplied by  $\mathbf{G}_1^\dagger$  and  $\mathbf{G}_2^\dagger$ , respectively, then  $\mathbf{Y}_1$  and  $\mathbf{Y}_2$  are obtained;

**Step 2:** From  $s_{1,1}=1$ , we get  $\hat{\mathbf{H}}^{(CP)}(0) = \mathbf{Y}_1^{(1,1)}$  and let  $i = 0$ ;

**Step 3:**  $i = i + 1$ ;

**Step 4:** For  $m = 1, \dots, M$  and  $r = 1, \dots, R$ , calculate

$$\hat{s}_{r,m}(i) = \frac{\text{vec}^H(\hat{\mathbf{H}}^{(CP)}(i-1)) \text{vec}(\mathbf{Y}_1^{(m,r)})}{\|\text{vec}(\hat{\mathbf{H}}^{(CP)}(i-1))\|^2};$$

**Step 5:** For  $n_D = 1, \dots, N_D$  and  $n_S = 1, \dots, N_S$ , calculate

$$\hat{h}_{n_D, n_S}^{(CP)}(i) = \frac{\text{vec}^H(\hat{\mathbf{S}}^T(i)) \text{vec}(\mathbf{Y}_2^{(n_D, n_S)})}{\|\text{vec}(\hat{\mathbf{S}}^T(i))\|^2};$$

**Step 6:** Let  $\gamma^{(i)} = \|\mathbf{Y}_1 - (\hat{\mathbf{S}}^T(i) \otimes \hat{\mathbf{H}}^{(CP)}(i))\|_F$ , if  $|\gamma^{(i)} - \gamma^{(i-1)}| \leq \delta_{\text{th}}$ , iteration completed. If not, repeat step 3-6.

In above procedures of the proposed algorithm,  $i$  denotes the iteration number. Since the proposed algorithm does not need to calculate the pseudo-inverse of matrix at each iteration, the proposed algorithm will not fall into local loop and convergence can be achieved through several iterations. It has low computational complexity.

## 6 Simulation Results and Discussion

The performance of the proposed semi-blind receiver is analyzed and verified by computer simulation results. The proposed receiver can effectively estimate the information symbols transmitted by the source node and channel matrices. Hence, we evaluate the bit error rate (BER) of symbols and the normalized mean square errors (NMSE) of channels to show the estimation performance. The NMSE of channels  $\mathbf{H}^{(SRD)}$  and  $\mathbf{H}^{(RD)}$  are defined as

$$NMSE(\mathbf{H}^{(SRD)}) = \frac{\|\hat{\mathbf{H}}^{(SRD)} - \mathbf{H}^{(SRD)}\|_F^2}{\|\mathbf{H}^{(SRD)}\|_F^2}, \quad (28)$$

$$NMSE(\mathbf{H}^{(SD)}) = \frac{\|\hat{\mathbf{H}}^{(SD)} - \mathbf{H}^{(SD)}\|_F^2}{\|\mathbf{H}^{(SD)}\|_F^2}, \quad (29)$$

where  $\hat{\mathbf{H}}^{(SRD)}$  and  $\hat{\mathbf{H}}^{(SD)}$  are the estimate of  $\mathbf{H}^{(SRD)}$  and  $\mathbf{H}^{(SD)}$ , respectively.

The elements in channel  $\mathbf{H}^{(SRD)}$  and  $\mathbf{H}^{(RD)}$  are independent and identically distributed complex Gauss random variables with mean value of 0 and variance of 1. QPSK modulation is used to transmit information symbols. In addition, we choose  $\delta_{\text{th}} = 1 \times 10^{-4}$  for the proposed algorithm, i.e., the iteration completed when  $|\gamma^{(i)} - \gamma^{(i-1)}| \leq 1 \times 10^{-4}$ . The BER of information symbols and the NMSE of channels  $\mathbf{H}^{(SRD)}$  and  $\mathbf{H}^{(RD)}$  are averaged 100,000 times by Monte Carlo runs.

We first evaluate the performance of the proposed semi-blind receiver with different extended code length. System parameters are set to  $N_S = N_{R_1} = N_{R_2} = N_D = 2$ ,  $R = 2$ ,  $M = 4$ . Fig. 2 and Fig. 3 show the

BER and NMSE performance of the proposed receiver under different extended code length. As can be seen from Fig. 2 and Fig. 3, the BER and NMSE of the proposed receiver decrease gradually with the increase of the length of the extended code. In Fig. 3, the NMSE of the direct link channel is higher than that of the relay auxiliary link channel. This is because the direct link has greater fading considering long-distance transmission. It can also be seen from Fig. 2 and Fig. 3 that the proposed algorithm still has good performance in signal detection and channel estimation even in the case of short extended code length ( $K = 4$ ).

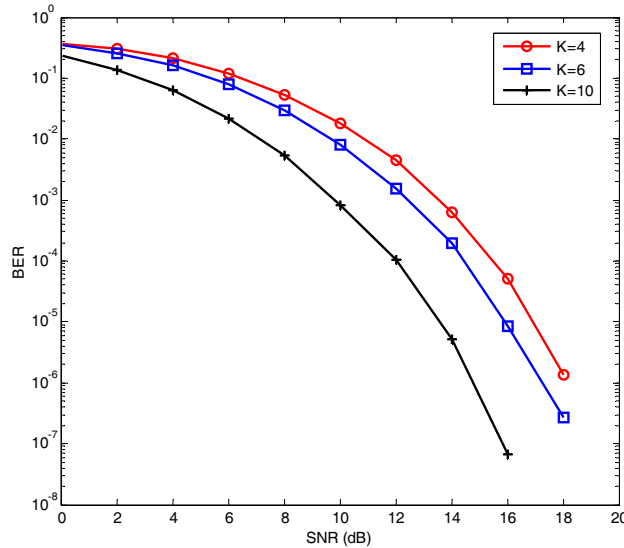


**Fig. 2.** BER performance of the semi-blind receiver with different extended code length

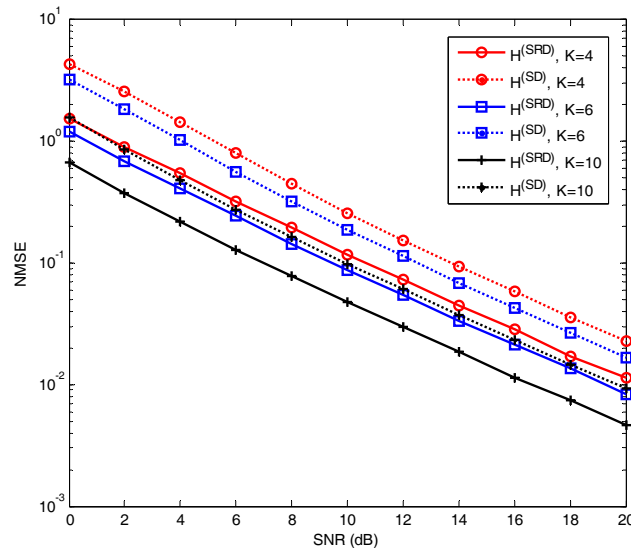


**Fig. 3.** NMSE performance of the semi-blind receiver under different extended code length

Secondly, the performance of the proposed receiver on the influence of data stream number and antenna number at the destination is considered. System parameters are set to  $N_S = N_{R_1} = N_{R_2} = 2$ ,  $K = M = 8$ . Fig. 4 and Fig. 5 show that the BER and NMSE of the proposed semi-blind receiver increase with the increase of data streams, but decrease with the increase of the number of antennas at the destination node. Traditional receivers require that the number of data streams must be equal to that of antennas at the source node. While the proposed receiver can arbitrarily choose the number of data streams. It can also be seen from Fig. 4 and Fig. 5 that the proposed semi-blind receiver still has high performance even when the number of data streams is larger than that of source antennas.



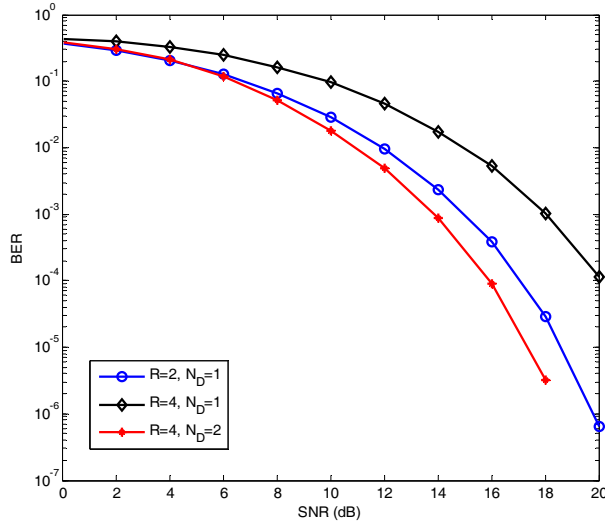


**Fig. 4.** BER performance of the proposed receiver with different number of data streams and destination antennas

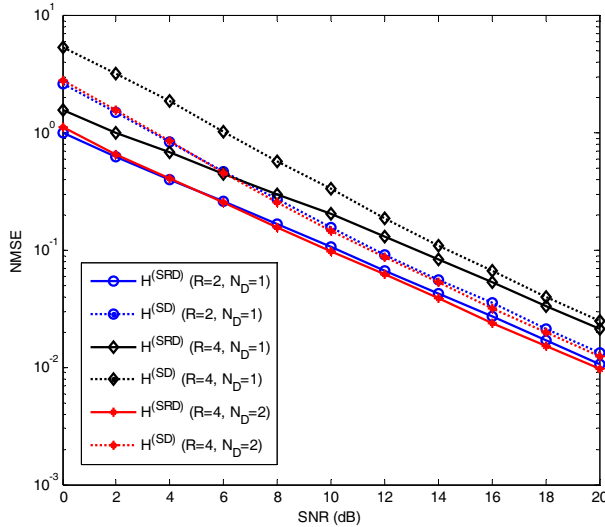


**Fig. 5.** NMSE performance of the proposed receiver with different number of data streams and destination antennas

Thirdly, the performance of the proposed receiver is compared with that of existing ALS receivers. System parameters are set to  $N_S = N_D = M = 4$ ,  $R = 2$ ,  $K = 8$ . Fig. 6 shows that the BER of the proposed semi-blind receiver and the existing ALS receiver decreases with the increase of the number of antennas at the relay node. Besides, the BER performance of the proposed receiver is better than that of the ALS receiver when  $N_{R_1} = N_{R_2} = N_R = 1$  and  $N_{R_1} = N_{R_2} = N_R = 2$ . The proposed receiver makes full use of the cooperative diversity gains, hence improves the estimation performance. Consistent with Fig. 6, Fig. 7 shows that the NMSE performance of the proposed receiver is better than that of the ALS receiver. In addition, Fig. 7 also shows that the proposed receiver can estimate not only the channel matrix of the relay auxiliary link, but also the channel matrix of the direct link.

Fourthly, we show the number of iterations required for the ALS receiver and the proposed receiver to converge in Table 1. It can be seen that with the increase of SNR, the number of iterations required for both receivers decreases gradually. Regardless of  $N_R = 1$  or  $N_R = 2$ , the iterations required for convergence of the proposed receiver is less than that of the existing ALS receiver. In addition, the proposed receiver converges only with a few iterations (3 times) in the case of medium and high SNR, which is a common scenario in practical communication. Therefore, the proposed receiver has lower computational complexity in practical communication.

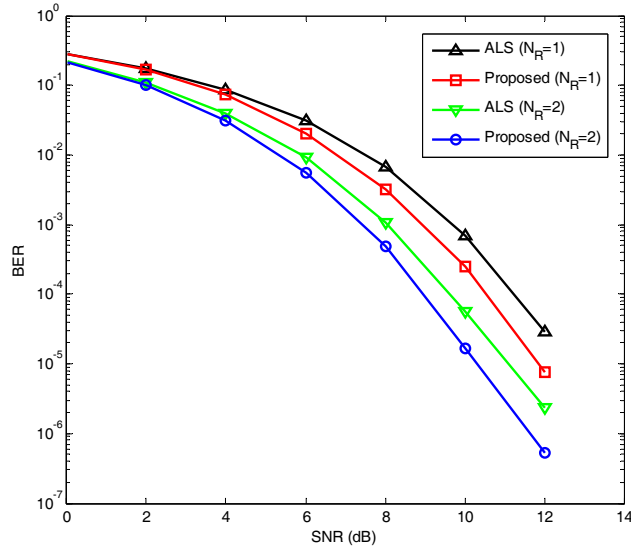


Fig. 6. BER performance comparison between the proposed receiver and existing ALS receiver

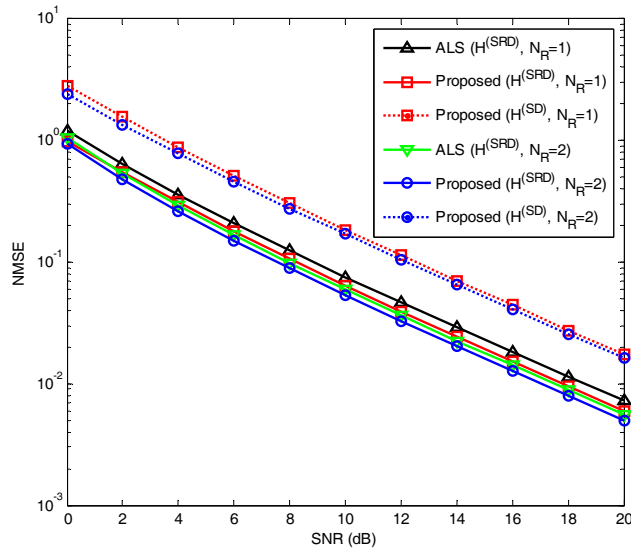


Fig. 7. NMSE performance comparison between the proposed receiver and existing ALS receiver

Table 1. The number of iterations required for convergence of ALS algorithm and the proposed algorithm

| SNR(dB)                   | 0 | 2 | 4 | 6 | 8 | 10 | 12 | 14 | 16 | 18 | 20 |
|---------------------------|---|---|---|---|---|----|----|----|----|----|----|
| ALS<br>( $N_R = 1$ )      | 8 | 7 | 6 | 5 | 5 | 4  | 4  | 4  | 4  | 4  | 4  |
| Proposed<br>( $N_R = 1$ ) | 6 | 6 | 5 | 4 | 4 | 3  | 3  | 3  | 3  | 3  | 3  |
| ALS<br>( $N_R = 2$ )      | 9 | 7 | 6 | 5 | 5 | 4  | 4  | 4  | 4  | 4  | 4  |
| Proposed<br>( $N_R = 2$ ) | 6 | 5 | 4 | 4 | 3 | 3  | 3  | 3  | 3  | 3  | 3  |

Finally, we consider the correlated channel scenario. The correlated channel models of channel matrices  $\mathbf{H}_w^{(SR)}$  and  $\mathbf{H}_w^{(SR)}$  can be expressed as follows:

$$\mathbf{H}_w^{(SR)}, \mathbf{H}_w^{(SR)}, \tag{30}$$

where the elements of  $\mathbf{H}_w^{(SR)}$  and  $\mathbf{H}_w^{(RD)}$  are the independent and identically distributed (i.i.d.) complex Gaussian random variable with 0 mean and variance 1, and  $\mathbf{A}_r = \mathbf{A}_r^{\frac{1}{2}} \mathbf{A}_r^{\frac{H}{2}}$ ,  $\mathbf{A}_t = \mathbf{A}_t^{\frac{1}{2}} \mathbf{A}_t^{\frac{H}{2}}$ ,  $\mathbf{B}_r = \mathbf{B}_r^{\frac{1}{2}} \mathbf{B}_r^{\frac{H}{2}}$ ,  $\mathbf{B}_t = \mathbf{B}_t^{\frac{1}{2}} \mathbf{B}_t^{\frac{H}{2}}$ . For simplicity, the correlation matrices are assumed to be  $\mathbf{A}_r = \mathbf{A}_t = \mathbf{B}_r = \mathbf{B}_t$  and  $\mathbf{B}_t(x, y) = \tau^{|x-y|}$ , where  $\tau$  is the normalized correlation coefficient. Fig. 8 and Fig. 9 respectively show the BER and NMSE performance curves of the proposed receiver and existing ALS receiver when the correlation coefficients are  $\tau = 0.2$  (weak correlation) and  $\tau = 0.8$  (strong correlation). As can be seen from Fig. 8 and Fig. 9, both of the BER and NMSE performance of the proposed receiver is better than that of the existing receiver. As the correlation of channel matrix enhances, the BER and NMSE performance of two receivers decrease correspondingly. However, the proposed receiver still has good estimation performance even in the strong correlation scenario.

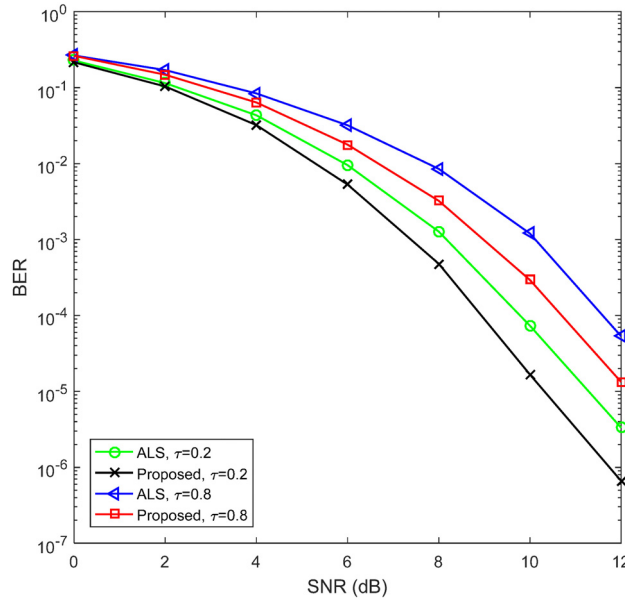


Fig. 8. BER performance of two receivers for correlated channels

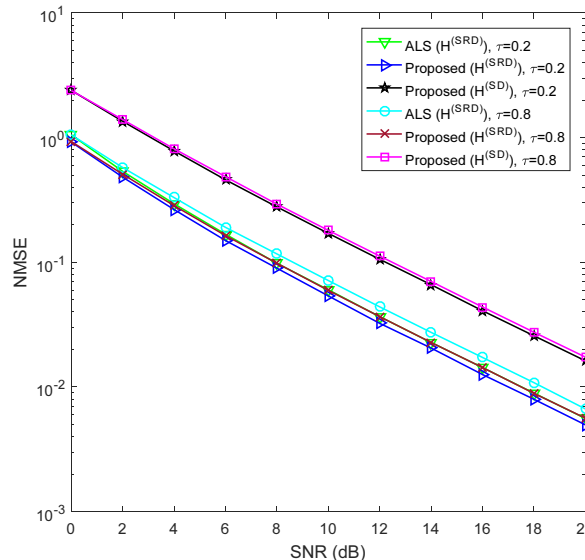


Fig. 9. NMSE performance of two receivers for correlated channels

## 7 Conclusion

In this paper, a semi-blind receiver based on Tucker-2 model is proposed for the cooperative MIMO relay system. The proposed semi-blind receiver utilizes the special structure of signal tensor. And then, an efficient fitting algorithm is designed to jointly estimate the information symbols and channel matrices of relay auxiliary link and direct link. The simulation results show that the proposed semi-blind receiver has higher estimation accuracy than the existing semi-blind receiver based on ALS algorithm. With the rapid development of communication technology, millimeter-wave massive MIMO relay system has become a research hotspot in academia. The next step is to consider extending the proposed receiver and applying it to the joint estimation of signals and channels in millimeter-wave massive MIMO relay system. In this system, the influence of channel sparsity on the proposed receiver will be considered and a higher accuracy fitting algorithm will be proposed.

## Acknowledgements

The authors thank the anonymous reviewers and the editor for their careful reviews and constructive suggestions to help us improve the quality of this paper. This work was supported by the grant from the National Natural Science Foundation of China (Nos. 61601414, 61701448, 61702466), the National Key Research and Development Program of China (No. 2016YFB0502001), and the Fundamental Research Funds for the Central Universities (Nos. CUC18A007, 2018CUCTJ082, 3132018XNG1808).

## References

- [1] Q. He, Z. Wang, J. Hu, R.S. Blum, Performance gains from cooperative MIMO radar and MIMO communication systems. *IEEE Signal Processing Letters* 26(1)(2019) 194-198.
- [2] J. Li, L. J. Cimini, J. Ge, C. Zhang, H. Feng, Optimal and suboptimal joint relay and antenna selection for two-way amplify-and-forward relaying, *IEEE Transactions on Wireless Communications* 15(2)(2016) 980-993. DOI: 10.1109/TWC.2015.2480850.
- [3] R. Zhao, H. Lin, Y. He, D. Chen, Y. Huang, L. Yang, Secrecy performance of transmit antenna selection for MIMO relay systems with outdated CSI, *IEEE Transactions on Communications* 66(2)(2018) 546-559. DOI: 10.1109/TCOMM.2017.2747554.
- [4] A. Papazafeiropoulos, t. Ratnarajah, Rate-splitting robustness in multi-pair massive MIMO relay systems, *IEEE Transactions on Wireless Communications* 17(8)(2018) 5623-5636.
- [5] B. Wang, J. Zhang, A. Host-Madsen, On the capacity of MIMO relay channels, *IEEE Transactions on Information Theory*, 51(1)(2005) 29-43.
- [6] Y. Yu, Y. Hua, Power allocation for a MIMO relay system with multiple-antenna users, *IEEE Transactions on Signal Processing* 58(5)(2010) 2823-2835.
- [7] P. Comon, Tensors: a brief introduction, *IEEE Signal Processing Magazine* 31(3)(2014) 44-53.
- [8] T. Kong, Y. Hua, Optimal design of source and relay pilots for MIMO relay channel estimation, *IEEE Transactions on Signal Processing* 59(9)(2011) 4438-4446.
- [9] J. Du, C. Yuan, J. Zhang, Low complexity PARAFAC-based channel estimation for non-regenerative MIMO relay systems, *IET Communications* 8(12)(2014) 2193-2199.
- [10] N.D. Sidiropoulos, L. De Lathauwer, X. Fu, K. Huang, E. E. Papalexakis, C. Faloutsos, Tensor decomposition for signal processing and machine learning, *IEEE Transactions on Signal Processing* 65(13)(2017) 3551-3582.

- [11] A. Cichocki, D. Mandic, L. De Lathauwer, G. Zhou, Q. Zhao, C. Caiafa, H.A. Phan, Tensor decompositions for signal processing applications: From two-way to multiway component analysis, *IEEE Signal Processing Magazine* 32(2)(2015) 145-163.
- [12] L.R. Ximenes, G. Favier, A.L.F. de Almeida, Y.C.B. Silva, PARAFAC-PARATUCK semi-blind receivers for two-hop cooperative MIMO relay systems, *IEEE Transactions on Signal Processing* 62(14)(2014) 3604-3615.
- [13] G. Favier, A.L.F. de Almeida, Overview of constrained PARAFAC models, *EURASIP Journal on Advances in Signal Processing* 2014(1)(2014) 142.
- [14] H.-Y. Lin, C.-W. Yuan, J.-H. Du, A fast algorithm with convergence for channel estimation in multi-user uplink amplify-and-forward relay system, *ACTA PHYSICA SINICA* 65(21)(2016) 21020. DOI: 10.7498/aps.65.210201.
- [15] J. Du, M. Han, Y. Hua, Y. Chen, H. Lin, A robust semi-blind receiver for joint symbol and channel parameter estimation in multiple-antenna systems, *Electronics* 8(5)(2019) 550.
- [16] L.R. Ximenes, G. Favier, A.L.F. de Almeida, Closed-form semi-blind receiver for MIMO relay systems using double Khatri-Rao space-time coding, *IEEE Signal Processing Letters* 23(3)(2016) 316-320.
- [17] W.C. Freitas, G. Favier, A.L.F. de Almeida, Sequential closed-form semiblind receiver for space-time coded multihop relaying systems, *IEEE Signal Processing Letters* 24(12)(2017) 1773-1777.
- [18] W.C. Freitas, G. Favier, A.L.F. de Almeida, Tensor-based joint channel and symbol estimation for two-way MIMO relaying systems, *IEEE Signal Processing Letters* 26(2)(2018) 227-231.
- [19] D. Lahat, T. Adali, C. Jutten, Multimodal data fusion: an overview of methods, challenges, and prospects, *Proceedings of the IEEE* 03(9)(2015) 1449-1477.
- [20] A.L.F. de Almeida, G. Favier, J.P.C.L. da Costa, J. Mota, Overview of tensor decompositions with applications to communications, in: R.F. Coelho, V.H. Nascimento, R.L. de Queiroz, J.M. Romano, C.C. Cavalcante (Eds.), *Signals and Images: Advances and Results in Speech, Estimation, Compression, Recognition, Filtering, and Processing*, CRC Press, Boca Raton, 2016, pp.325-356.
- [21] J.D. Carroll, S. Pruzansky, J.B. Kruskal, CANDELINC: a general approach to multidimensional analysis of many-way arrays with linear constraints on parameters, *Psychometrika* 45(1)(1980) 3-24.